Hajri sondes
Ben Amor Abdessattar
Gasmi Moncef

J. Electrical Systems x-x (xxx): x-xx

Regular paper

Improvement Characterization Resulting from the Losses Reduction in a Linear Stepping Motor

In this paper we want to satisfy two objectives. The first objective consists on the improvement of Joule losses by modification of dental geometrical dimensions. We had proceeded by simulation, using CAO software "MATLAB" that identified the losses variations as a function of the dental geometrical dimensions. So that, the analysis of the obtained results, had leaded to extract the best appropriate dimensions of tooth and slit widths. The second objective consists on Joule losses reduction by the decrease of magnetomotive force. Then the proposed structure, taking account the new dental dimensions, had considered a migration from the existing reluctant structure to a hybrid more perfect one. The obtained simulation results, of the induction in the teeth and slits sharp extremities, had showed an important local induction saturation that had leaded to introduce some adjustments on these extremities forms in order to limit this insufficiency.

Keywords: Joule losses, Force, toothed structure, magnetomotive force, clutter, overheats, local saturation

1. INTRODUCTION

The heating, in an electric machine, is a very important factor that, often lead to the destruction of its constituents and limit eventual magnets functioning [1, 2]. Joule losses, created in coils, and iron losses created in the magnetic circuits, are essentially the origin of electric machine heating [1, 3, 4, 5]. Hence, several researchers have oriented their efforts for reducing losses in actuators to avoid their effects [6, 7, 8, 9].

Yet, linear electromagnetic actuators, frequently, suffer from a low force-to-volume ratio [10, 11, 12]. In general, to increase this ratio various approaches have been considered, where the number of poles is increased or the polar step is reduced [2], and some others had considered new structures based on multiplying air gap [2], or on introducing this criteria since the design phase [1, 10, 13]. So, the new progressive approach presented in this paper will permit to reduce the machine heating and will contribute to improve the force-to-volume ratio in a prototype of a linear brushless tubular stepping motor.

The proposed approach presents two complementary steps. In the first step, Joule losses reduction has been resulted next to the modification of horizontal geometric parameters dimensions with considering constant the dental step. So, that the dimension increase of slit width has been followed by the reduction of tooth width.

In the second step, and in order to more ameliorate Joule losses with respecting the required maximal force value, we had proposed a reluctant polarized structure. The permanent magnets addition will influence on the motor performances.

The new parameters are retained to continue the studies concerning the clutter, the force-to-losses ratio and the electric machine heating.

Finally, we present induction simulation results in the extremities of teeth and slits using geometrical modification to limit the local induction saturation.

2. STRUCTURE OF THE EXISTING PROTOTYPE

Corresponding author : Hajri sondes
Ecole Nationale d'Ingénieurs de Tunis, (ENIT), Tunisia hajri_sondes@yahoo.fr

The existing prototype of motor presented by figure (1) is a brushless linear tubular step-by-step motor, with switched reluctance.

Fig.1.The ancient laboratory prototype

The stator includes four similar modules. Stator and mobile part had a toothed structure.
Each of these modules is formed of a magnetic circuit made of soft Steel and a coil made of copper and lodged in the notch of stator magnetic circuit.
Figure (2) presents a cut of the existing motor. The stator's four modules are identical. Each of them has an exterior diameter 90mm.
Tooth and slit have similar dimension, for the stator and the mobile part, equals to 5,08mm.
Each module is separated from the second one by a strut of width 2,54mm.

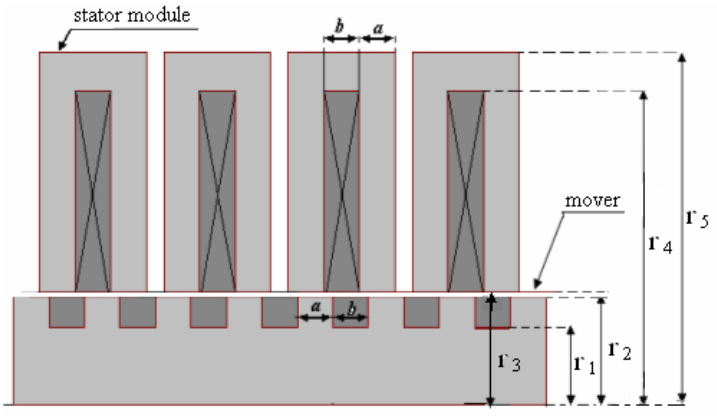

Fig.2. Geometrical parameters of the existing motor

3. JOULE LOSSES ANALYSIS

Many researchers are interested by the reduction of losses [1, 7, 15]. We will begin by extracting the influential parameters described by Joule losses expressions relative to the studied stepping motor. Then, we proceed by analytic study to determine the factors that penalise these kinds of motor.

3.1. Joule losses impacts

Joule losses are the most major ones in an electric machine, they are created in coils. These losses p_J, expressed by (1), are functions of the coil average resistance R and the current i

[3, 12, 14, 22].

$$p_J = R \cdot i^2 \tag{1}$$

Relative to the considered existing motor, the coil overage resistance is expressed by [1, 12, 17, 22]:

$$R = \frac{\rho_c \, l_{moy}}{S_f} \cdot N \tag{2}$$

ρ_c is the copper resistivity;

l_{moy} is the spire middle length;

N is the coil spires number;

S_f is the copper wire section.

The spire middle length l_{moy} is a function of the coil exterior radius r_4 and the coil interior radius r_3:

$$l_{moy} = \pi \times (r_4 + r_3) \tag{3}$$

When the coil interior radius r_3 is constant, the coil exterior radius r_4 will be given by:

$$r_4 = \frac{S_b}{b} + r_3 \tag{4}$$

With S_b is the winding area obtained by:

$$S_b = \frac{N \cdot S_f}{k_b} \tag{5}$$

k_b is the winding coefficient.

Then the coil exterior radius can be written:

$$r_4 = \frac{N \cdot S_f}{k_b \cdot b} + r_3 \tag{6}$$

Considering the expressions (1), (2), (3) and (6), Joule losses will be expressed by:

$$p_J = \left(\frac{\rho_c \cdot \pi}{k_b} \right) \cdot N^2 \cdot i^2 \cdot \frac{1}{b} + \left(\frac{\rho_c \cdot \pi \cdot 2r_3}{S_f} \right) \cdot N \cdot i^2 \tag{7}$$

i is the alimentation current.

The reduction of Joule losses can be given by increasing the slit width b or by reducing the spires number N and the current value.

The reluctant system maximal force depends on the spires number and the current value. For the considered motor this force F_{max} is given by [21]:

$$F_{max} = \frac{N^2 \cdot i^2 \cdot \pi}{\lambda} \cdot \left(\frac{P_o - P_a}{2} \right) \tag{8}$$

λ is the dental step;

P_o is the teeth opposition position permeance;

P_a is the teeth alignment position permeance.

$$P_o - P_a = \mu_0 \cdot L_d \cdot K_F \tag{9}$$

μ_0 is the vacuum magnetic permeability;
K_F is the force coefficient, it can be computed by application of approached analytic method permitting to calculate the airgap characteristic functions [21];
L_d is the airgap perimeter, given by:

$$L_d = 2\pi r_e \tag{10}$$

r_e is the airgap medium radius.

Then, considering the relations (8), (9) and (10) the maximal force expression will be written:

$$F_{max} = \frac{\mu_0 \cdot \pi^2 \cdot r_e \cdot K_F \cdot N^2 i^2}{\lambda} \tag{11}$$

The maximal force value required by the application is fixed to 20N. To consider this value we need to maintain the magnetomotive force constant relative to the values of spires number N and current i. Then, the suitable solution to reduce Joule losses, with maintaining constant the maximal force value, consists in geometrical parameter control.

3.2. Geometrical parameters control

Considering that the spires number N and the current value are constants, Joule losses p_J can be written as a function of the slit width 'b':

$$p_J = A \cdot \frac{1}{b} + C \tag{12}$$

Where, A and C are two constants described by:

$$A = \rho_c \cdot \pi \cdot \frac{N^2}{k_b} \cdot i^2 \text{ and } C = \rho_c \cdot \pi \cdot 2r_3 \cdot \frac{N}{S_f} \cdot i^2$$

We notice, from (12), that p_J are inversely proportional to the slit width 'b'. This geometrical parameter 'b' is in correlation with the tooth width 'a' by:

$$a + b = m\lambda_e = \lambda \tag{13}$$

m is the stator modules number, and λe is the elementary mechanical step.

Then Joule losses reduction can be done by control of the geometrical parameter 'a' and 'b'. Figure 3 shows the Joule losses variations as a function of the slit width 'b'.

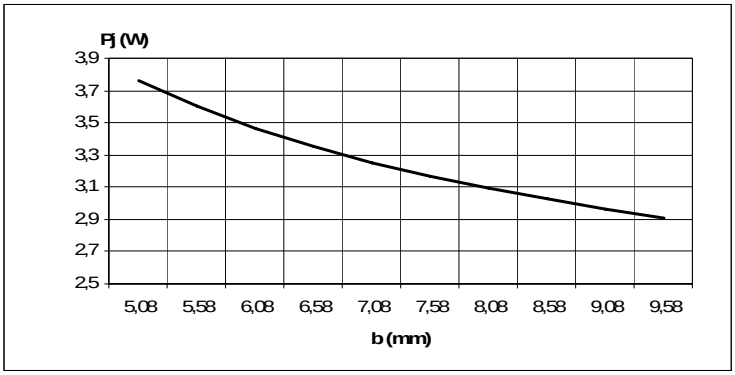

Fig.3. Joule losses as a function of slit width 'b'

To limit these dental parameters, we have to take account the magnetic saturation constraint of the used material.

The maximal induction B_{mi} in a section S_i of a magnetic circuit iron part can be written as:

$$B_{mi} = \frac{\phi_m}{S_i} \tag{14}$$

ϕ_m is the maximal magnetic flux crossing the magnetic circuit iron sections and the airgap surface, it is constant. The sections S_i decrease with the tooth width attenuation, so the maximal induction B_{mi} will be increased.

The magnetic constraint imposes the level of inductions top values. So, several numerical simulations using finite elements software "MAXWELL" had served to obtain the optimal dimensions reducing Joule losses.
Figure 4 presents a finite elements model of the studied stepping motor and describes a solution mesh for computing the magnetic flux density by finite elements method.

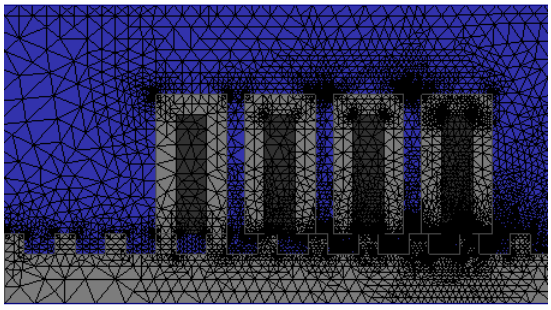

Fig.4. Finite elements model of the studied stepping motor

Magnetic constraint

For the choice of magnetic circuit measurements we have considered a level of induction achieving a compromise between the technical constraints and the economic aspects [3]. In fact, we have to work in a level of induction inferior to the saturation limit and we have to reduce the iron volume.

Considering the iron material $FeCo_{50\%}$ chosen in previous work [23] for the construction of the studied stepping motor, the induction saturation limit situated in the extreme part of the induction curve linear domain is equal to 2,4T.
Numerical simulations had given the induction values in different points of magnetic circuits for different horizontal dimensions.
Figure 5 gives an example of these simulation results, where the slit width 'b' is equal to the tooth width 'a' (a=b=5,08mm).

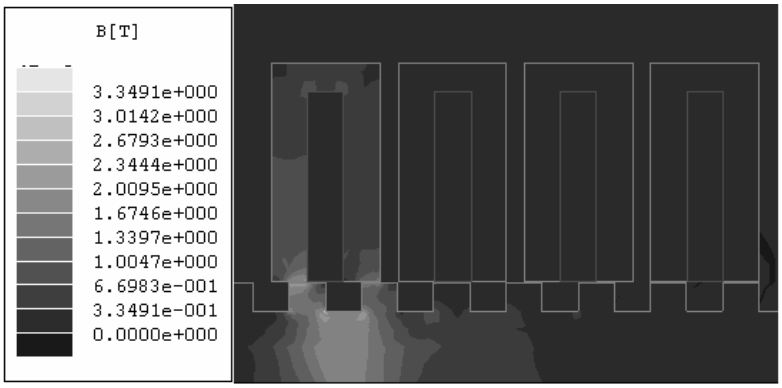

Fig.5. Induction in a magnetic module for a=b=5.08mm

The colours graduation illustrates the various induction levels relative to the different parts of the motor module. We mark from this figure that the maximal induction level is situated in the airgap. Then the airgap induction value must be inferior to 2.4T.

Variation of induction in the airgap

We had to simulate the induction in the airgap for different values of the geometrical parameters 'a' and 'b'.
Figure 6 shows the induction variation in the airgap according to the tooth width 'a'.
We notice that the induction values in the airgap increase when the tooth width values decrease. For *a*=3,96mm the airgap induction value is equal to 2,4T. The relation (13) permits to determine the corresponding slit width value b. The couple (a, b) = (3,96mm, 6,2mm) will be retained to continue this work.

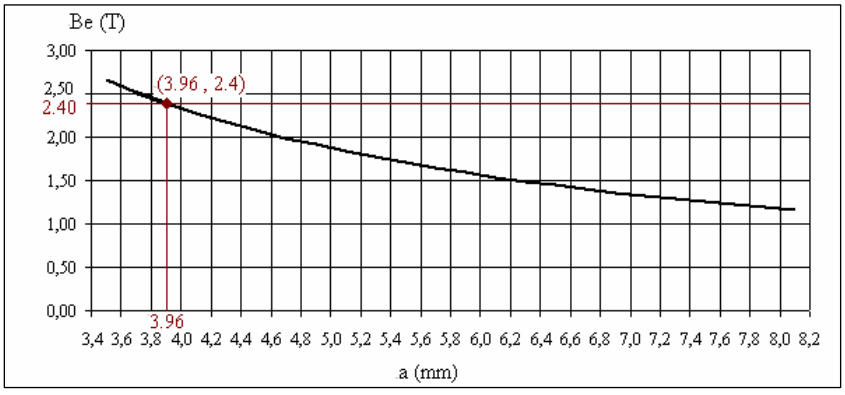

Fig.6. Induction airgap values according to the tooth width

3.3. Electric parameters control

Another method reducing Joule losses with maintaining constant the maximal force value consists in transforming the reluctant system to a reluctant polarized one.

In fact, to correct the force decrease, resulting to the spires number or the current values reduction, we project to insert permanent magnets in the motor stators.

In the case of a reluctant polarized system, the global developed force is given by [3, 14, 17, 18] as:

$$F = \frac{1}{2}\left(\frac{\Delta P_{aa}}{\Delta x}\theta_a^2 + \frac{\Delta P_{bb}}{\Delta x}\theta_b^2 + 2\frac{\Delta P_{ab}}{\Delta x}\theta_a\theta_b \right) \quad (15)$$

θ_b, θ_a are the coil and the magnet magnetomotive forces;

P_b, P_a are the coil and the magnet permeances;

P_{ab} is the mutual permeance;

x is the displacement.

This force is the sum of the force F_b generated by the coil, the force F_a generated by the permanent magnets and the mutual force F_{ab} that can be expressed as:

$$F = F_a + F_b + F_{ab} \quad (16)$$

The new proposed structure with permanent magnets can be able to improve the generated force.

Numerical flux simulation results had leaded us to retain the structure with a stator magnets emplacement. Figure 7 shows the proposal system that permit to maintain the majority of flux lines concentrated through the same module. The new developed force, generated by the new reluctant polarized system, has improved 1.75 times.

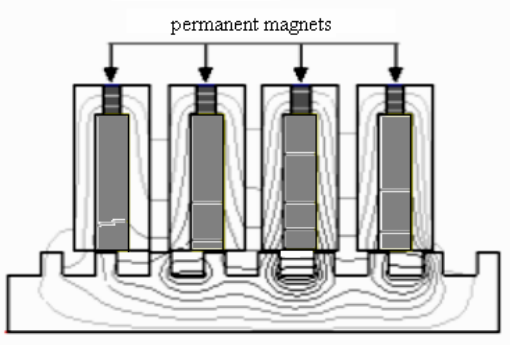

Fig.7. New reluctant polarized structure

To choose the permanent magnets material we had studied the characteristics of three well-known magnet materials: 'Alnico', 'Samarium-Cobalt' (S_mC_o) and 'Neodyme-Fer-Bore' (N_dF_eB) [3, 10, 12, 19].

The type choice of the magnets material depends on the kind of the application. In fact, there are dilemma cost/performances to consider. Therefore, in this context, we are

interested by the highness of the developed force.
The simulation results, using MAXWELL software, concerning the three considered materials, had entailed to the maximal force values presented in table 1.

Table1: Maximal forces generated for different magnet materials

Permanent magnet materials	Alnico	S_mC_o	N_dF_eB
F_{max} (i=0.48A) (N)	35.63	41	43,9N

These results show that the N_dF_eB permanent magnet material generates the best maximal force.

In addition, Maxwell simulations had been used on the three considered permanent magnet materials to extract the current value corresponding to the required maximal force (20N), for the initial spire number. Figure 8 shows the corresponding results.

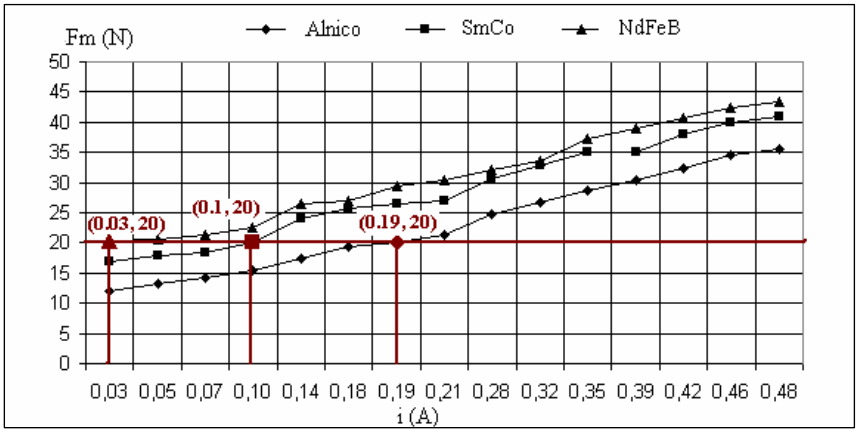

Fig.8. Maximal force as a function of the current i

This figure shows that the use of the N_dF_eB permanent magnet material permits to generate the required maximal force (F_{max}=20N) with a minimal current value equal to 0,03A.

The presented results advantage the choice of N_dF_eB permanent magnet material, so we will retain this material for the manufacturing of the prototype.

Numerical simulations applied on the N_dF_eB permanent magnet material for different magnetomotive forces values permit to extract the value relative to the required maximal force, which is equal to 50Atrs.

Then, the reduction of the magnetomotive force value, will necessary influence on Joule losses values. Table 2 presents a comparison of Joule losses during the different design steps.

Table 2: Evolution of Joule losses during the design steps

Steps	step1	step2	step3
p_J (W)	4.77	3.4	0,013

step1: The initial conception of the existing motor,
step2: The modification of geometrical parameter, b=6,2mm.
step3: The adopted form for Ni=50Atrs.

4. CHARACTERISTICS IMPROVEMENTS

The new approach applied to reduce Joule losses entails some advantages to the studied stepping motor. The most important advantage consists in the clutter reduction

The equation (6) shows that the radius r_4 depends on the spires number N and it is inversely proportional to the slit width b. The exterior radius r_5 of the motor is the sum of the radius r_4 and the breech thickness e_c. Figure 9 shows the variation of the exterior radius r_5 according to the variation of slit width b.

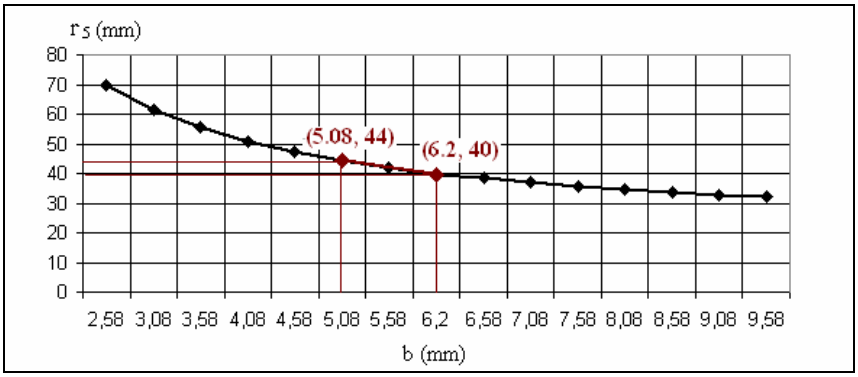

Fig.9. Exterior radius r_5 as a function of slit width "b"

We note that the exterior radius of the motor will be reduced by the increase of the slit width of the stator and the movable part. This exterior radius is more reduced by the decrease of the spires number N entailed by the magnetomotive force reduction. The action realized in order to reduce Joule losses had allowed the clutter reduction.
In addition, the clutter reduction, the tooth width minimization and the spires number reduction had contributed to reduce the volumes of the used iron and copper. Figure 10 illustrates the ancient (1) and the proposed (2) structures.

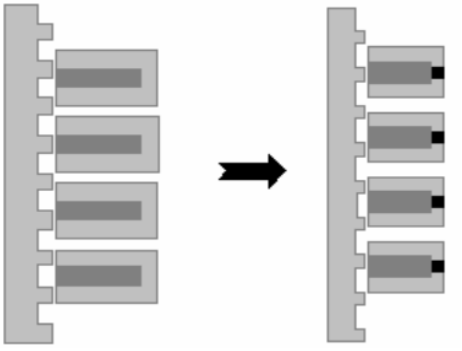

(1) Ancient structure (2) Proposed structure

Fig.10. Comparison of the existing and the proposed structures

In an electric motor, losses entail the motor components overheat. An excessive overheat

can lead to the deterioration of the coil insulator and to the demagnetization of eventual magnets. Therefore, the modifications, made in the new motor design in order to reduce losses will necessary attenuate the motor overheat.

5. AMELIORATION OF EXTREMITIES AND CORNER FORMS

In this part we present some propositions of form and measurement changes that can lead to the improvement of the studied stepping motor characteristics. In order to determine the most appropriate form, avoiding the local induction saturation at the corners, we have applied the test-error method using MAXWELL simulation software.

5.1. Extremities of teeth

Figure 11 shows the magnetic induction saturation in tooth extremities (B≈ 2,76T) obtained by MAXWELL simulation results.

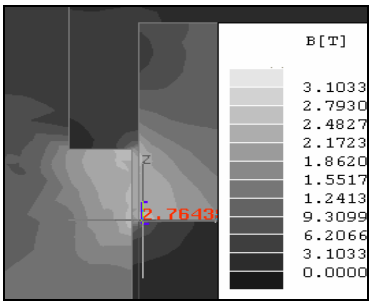

Fig.11. Saturation in tooth extremities (B=2.76T)

To avoid the local saturation in tooth extremities we had proposed two different extremity forms, curved and triangular. The induction simulation results relatives to these proposed forms are illustrated by figure 12.

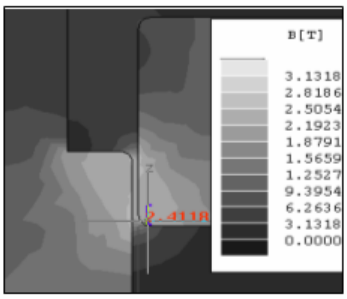

(1) Curved extremities (B=2.41T)

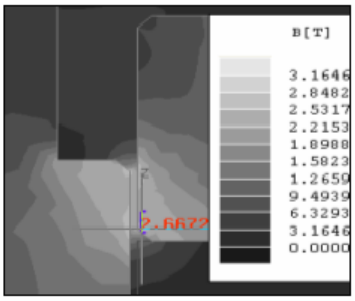

(2) Triangular extremities (B=2.66T)

Fig.12. Comparison of two proposed extremity forms

These results encourage the choice of the curved extremity form that permits to more reduce the induction saturation (from 2.76T to 2.41T).

5.2. Corners of the mobile part slit

Figure 13 shows the magnetic induction in corners of the mobile part slits. It presents a local saturation B≈3T.

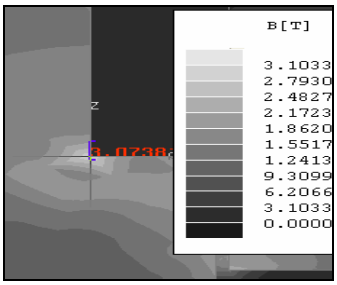

Fig.13. Induction saturation in the corner slit (B=3T)

To attenuate the value of saturated magnetic induction, we have proceeded by realizing curved and triangular corners (Fig.14).

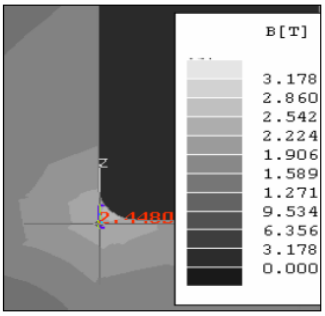

(1) Curved corner (B=2.44)

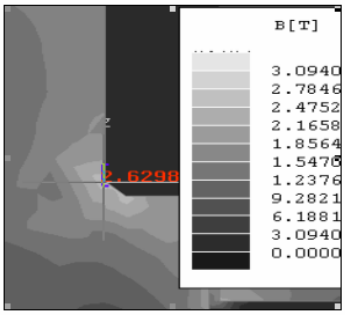

(2) Triangular corner (B=2.62)

Fig.14. Comparison of two proposed corner forms

These results advantage the choice of curved corner form which permits an appreciable reduction of induction saturation in these regions (from 3 to 2.44T).

5.3. Curve measurements

The choice of the most appropriate curve measurements necessities the realization of curves having different values of quote c (Fig.15).

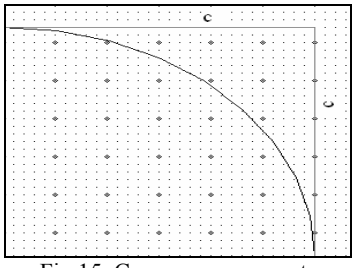

Fig.15. Curve measurements

The induction simulations in the realised curves of different measurements entail the results presented in figure 16.

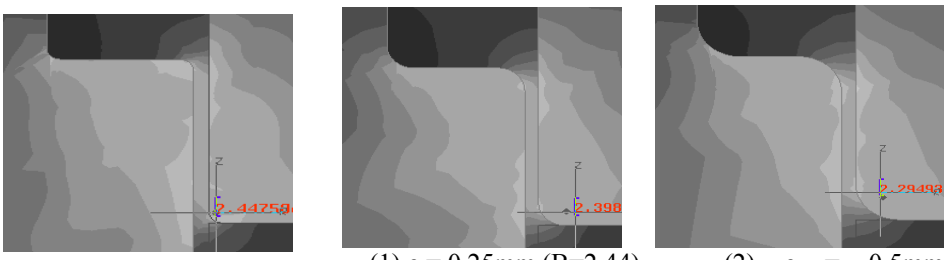

(1) c = 0.25mm (B=2.44) (2) c = 0.5mm (B=2.39) (3) c = 1mm (B=2.29)

Fig.16. Results of induction simulations relative to different curve measurements

It is clear from figure 16 that more the curve quote is large more the induction saturation decrease.
Simulations of the magnetic induction, in all tests, encourage the choice of curve of quote 1mm. This choice permits the disappearance of the local saturation but it entails a big modification of the tooth height equal to 4mm that increase the leakage flux lines. Then it is most appropriate to choose the quote equal to 0.25mm.

6. CONCLUSION

In this paper, a method for improving a stepping motor prototype design is presented. The analysis of Joule losses and force insufficiencies has permit to manage the geometric dimensions and to transform the ancient reluctant system in a reluctant polarized system.
Also, Several numerical simulations results, based on the electromagnetic constraint analysis had showed the influence of the dental ratio on the saturation and clutter reduction.
In order to more ameliorate the studied motor we have proposed some solutions based in numerical simulations. The new proposed motor, resulting of these studies has curved extremities of teeth and corners.

REFERENCES

[1] E. Hoang, Etude, modélisation et mesure des pertes magnétiques dans les moteurs à réluctance variable à double saillance, Ph D. Thesis, E N S Cachan, December, 1995.

[2] P.E. Cavarec, H. Ben Ahmed, B. Multon and L. Prévond, Avantage of increasing the number of airgap surfaces in synchronous linear actuator, International Conference Electromotion'01, Poland, pp.251-256, 19-20 June 2001.

[3] M. Jufer, Electromécanique, Treaty about Electricity, Electronics and Electrotechnics, Ed Georgi Dunod, 1979.

[4] N. Kutkun and J. Anthony, A simplified method for estimation of iron loss in wound toroidal cores energized by pulse width modulated voltage sources, Journal of Magnetism and Magnetic Materials, Vol. 284, pp.195-200, December 2004.

[5] S. Hajri, A. B. Amor and M. Gasmi, Improvement of force-to-losses ratio for a linear stepping motor, International Conference iceedt'07, Tunisia, 2007.

[6] A.T**.** Wilder, Characterization of power losses in soft magnetic materials, IEEE presse ISBN 0-7803-9259, 2005.

[7] P**.**E. Cavarec**,** H.B. Ahmed and B. Multon, Improvement of the magnetic core for eddy current losses decreasing in cylindrical linear actuators, International Conference ISEM'03, 12-14 May 2003.

[8] D. Lin, P. Zhou and W.N. Fu, A dynamic core loss model for soft ferromagnetic and power ferrite materials in transient finite element analysis, IEEE. Magnetic Transaction, Vol. 40, No.2, pp.1318-1321, March 2004.

[9] S. Hajri, A.B. Amor and M. Gasmi, Approche de réduction des pertes par analyse de l'influence des parameters de construction d'un moteur pas à pas linéaire, International Conference STA'07, Tunisia, 2007.

[10] H.B. Ahmed, J. Lucidarme and P. F. Desesquelles, Méthode semi-numérique de pré-dimensionnement des machines à aimants permanents et à bobinage global, Journal Physic III. France 5, pp.703-725, 1995.

[11] L. Elamraoui, F.Gillon, P. BROCHET and M. B. REJEB, Performance estimation of linear tubular actuators, International Conference MAGLEV'02, Lausanne, 2002.
[12] S. Chevailler, Comparative study and selection criteria of linear motors, D. Thesis, Federal Polytechnic School of Lausanne, July 2006.
[13] H.B. Ahmed, B. Multon and P.E. Cavarec, Actionneurs linéaires directs et indirects: performances limites, Journal Club EEA, University Cergy-Pontoise, 2003.
[14] G. Grellet and G. Clerc, Actionneurs Electriques, Ed Eyrolles, Paris, 2000.
[15] Y. Amara, J. Wang and J. Howe, Influence of soft magnetic materials on the design and performance of tubular permanent magnet machines, IEEE Transactions on Magnetics, Vol. 41, N° 10, pp.4057-4059, October 2005.
[16] A.B. Amor, S. Hajri and M. Gasmi, Optimization of a linear stepping motor force by geometrical parameters control, International Conference CPI'07, Maroc Rabat, 2007.
[17] P. Maye, Moteurs électriques pour la robotique, Ed Dunod, Paris, 2000.
[18] D. Matt and J. F. Libre, Performances comparées des machines à aimants et à reluctance variable. Maximisation du couple massique ou volumique, Journal Physics III France 5, N°10, pp 1621-1641, Octobre 1995.
[19] F. L. Ringuet, Aimants permanents, Matériaux et applications, Techniques de l'Ingénieur, traité Génie électrique, 1995.
[20] A.B. Amor, S. Hajri and M. Gasmi, Characteristics improvement of a brushless linear motor, International Conference ICSSSMO07, Chine, 2007.
[21] P. Favier, Contribution à la conception et à la commande de machines à reluctance variable linéaires destinées à l'amortissement et au contrôle des systèmes mécaniques vibrants, D. Thesis, University of sciences et techniques, Lille Flandre-Artois, Jun 1988.
[22] S. Hajri, A.B. Amor and M. Gasmi, Approche de conception améliorée d'un moteur brushless linéaire, Fourth International Conference JTEA'06, Tunisia, 2006.
[23] S. Hajri, A.B. Amor and M. Gasmi, Caractérisation de matériaux et modélisation des pertes fer dans une machine réluctante, International Conference CRATT'07, Tunisia, 2007.